



System for Automatic Diabetic Retinopathy

^[1]Orken Mamyrbayev, ^[3]Kymbat Momynzhanova, ^[2]Sergii Pavlov,
^[2]Lubov Zagoruyko, ^[1]Dina Oralbekova, ^[3]Sholpan Zhumagulova

¹Institute of Information and Computational Technologies, Almaty, 050010, Kazakhstan, morkenj@mail.ru, dinaoral@mail.ru

²Vinnitsia National Technical University, Vinnitsia, 21000, Ukraine

psv@vntu.edu.ua,

³Kazakh National University, Faculty of Information Technology, Almaty, 050038, Kazakhstan
kymbat010809@gmail.com, shzhumagulovakz@gmail.com

Volume 6, Issue 15, Sep 2024

Received: 15 July 2024

Accepted: 25 Aug 2024

Published: 05 Sep 2024

[doi: 10.48047/AFJBS.6.15.2024.7898-7902](https://doi.org/10.48047/AFJBS.6.15.2024.7898-7902)

Abstract— *Glaucoma is an incurable disease that leads to vision loss. Early diagnosis and detection of this pathology provide an advantage in slowing the progression of glaucoma. Accurate segmentation of the optic disc (OD) and optic cup (OC) is useful for diagnosing glaucoma. In recent years, deep learning has achieved remarkable results in the segmentation of OD and OC. However, OC segmentation is more challenging than OD segmentation due to the high variability in shape and unclear boundaries, which reduces the performance of models for detecting and segmenting the OC.*

This study examines methods for processing fundus images to identify glaucoma pathology, localize it, and analyze its changes over time, which is crucial for accurate diagnosis. The method of fundus image registration and mathematical models play an important role in describing fundus images. The image space model, in particular, provides powerful analytical tools for studying these images.

Further image processing is based on neighboring pixels, allowing precise transformation of images based on brightness values in localized areas.

IndexTerms— *glaucoma, neural network, image preprocessing, classification, medical diagnosis.*

I. INTRODUCTION

Glaucoma is the second leading cause of irreversible blindness worldwide after cataracts and refractive errors, accounting for nearly 8% of global blindness. The global incidence of glaucoma was more than 60.5 million people in 2020 and is estimated to reach 80 million by 2025 and 111.8 million by 2040. India has the highest rate - 23.5%. In Europe, 7.8 million people suffer from glaucoma, and the overall prevalence is 2.51%.

The most common type of glaucoma in the UK is primary

open-angle glaucoma (OPEG), affecting 2% of people over 40 and 10% of people over 75, particularly of Afro-Caribbean descent; PVOG is not so common among people younger than 40 years and affects only 0.17% of people.

The prevalence of glaucoma increases with age and thus may be associated with age-related conditions such as macular degeneration, vascular disease, and obstructive sleep apnea. Its prevalence is highest among older Hispanics (18%), blacks (15%), whites (7%), and Asians (5%). Finally, there are also gender differences in glaucoma: the prevalence of glaucoma is 36% higher in men than in women [1].

Glaucoma is a neuropathic disease characterized by

degeneration of ganglion cells [2, 3]. Thus, atrophy of the optic nerve fiber is accompanied by erosion of the tissue of the rim, which is manifested by cupular expansion. Today, detection of glaucomatous structural damage and changes is one of the most difficult aspects of disease diagnosis methods [4, 5]. In addition, glaucoma is usually diagnosed by measuring the intraocular pressure (IOP), which should be greater than 22 mm Hg. Art. without treatment, glaucomatous cupping of the optic disc and glaucomatous visual field defects [3].

II. DESCRIPTION OF THE PROBLEM OF DIAGNOSING GLAUCOMA IN AUTOMATIC MODE

One of the biggest problems in the diagnosis of glaucoma is the asymptomatic aspect of the disease before the severe stages. Thus, the number of undiagnosed patients exceeds the number of diagnosed ones [6]. However, the size and shape of

the optic disc is another important aspect that should be taken into account when diagnosing glaucoma [7]. Therefore, the vertical increase of the cup is a sign of glaucomatous neuropathy of the optic nerve. When analyzing the image of Fig. 1 c, d, it turns out from enlargement of the cup compared to Fig. 1 a and b. This is a clear sign of glaucoma [8].

Processing of glaucoma images for the purpose of identification of pathology, its localization and analysis of the dynamics of changes in automatic mode is an extremely important element of diagnostics. Neural networks are widely and effectively used to solve image processing and recognition problems. In this intensively developing area of research, new tasks are constantly appearing, related to the development of new structures of deep neural networks, the purpose of which is to increase the probability of diagnostic information with full automation of the diagnostic procedure. The article proposes and investigates a method of obtaining images of the fundus, methods of preprocessing images for further training of a neural network for the identification and classification of pathologies.

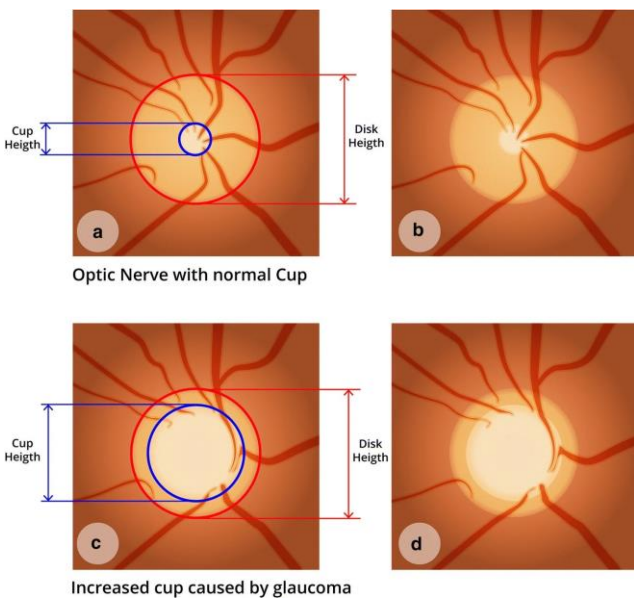


Figure 1. Optic nerve with normal cup and enlarged cup caused by glaucoma: where a, b - optic nerve with normal cup and dimensions;

c, d - optic nerve with an enlarged cup

III. METHOD OF REGISTRATION OF FUNDUS IMAGES

Solving the tasks of processing complex glaucoma images, for which the issues of image segmentation and formal description of its parts for correct recognition are relevant, the research of new methods of neuro-like processing and the development of neural networks with deep learning and subsequent analysis of the results for a compact presentation of data with greater flexibility in the selection and processing of features while maintaining their simplicity and noise resistance are relevant.

A method of registering images of the fundus was developed to study the problems of diagnosing glaucoma. The device that implements the method of obtaining, identifying and storing images of the fundus is a smartphone based on the Android operating system. Structural scheme of the method submitted in Fig. 2.

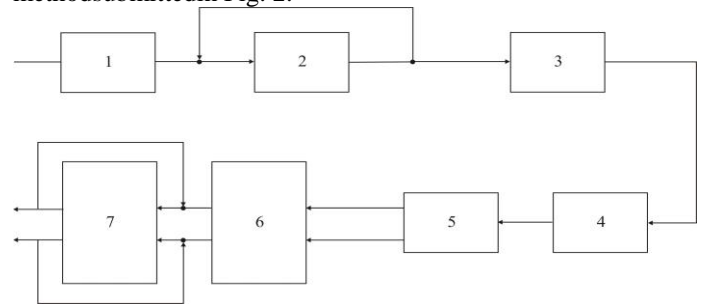


Figure 2. Block diagram of the method of registration of fundus images

The initial image is registered by the smartphone camera 1 and using the JfaceDetector_Face function [9] in block 2 the face is identified and the midpoint of the face is calculated using the SrcFace.getMidPoint(Point) function and the distance between the eyes D using the SrcFace.eyesDistance function.

Next, in block 3, the eye position is calculated based on the midpoint of SrcFace and the distance between the eyes:

$$d_L = f(x - 0.5 * D, y), \quad (1)$$

$$d_R = f(x + 0.5 * D, y), \quad (2)$$

where f is a vector of point positions in the x, y plane;

D- the distance between the eyes;

dL –the position of the left eye;

dR is the position of the right eye.

You can also use function SrcFace.pose to perform rotation eye position around the center, however, on most Android devices Pose always returns 0.

Blocks 4 and 5 perform image scaling and rotation (if necessary) for further diagnosis. The left and right images enter the input of block 6 eye. In this block image processing is performed left and right eye in order to register the fundus by applying a filter (monochromatic, color, pixel, etc.). Block 7 performs the search for the optimal solution for detecting the signs of glaucoma and further classification of the disease.

IV. MATHEMATICAL MODELS OF FUNDUS IMAGE REGISTRATION AND PROCESSING

One of the mathematical models for describing images is to assign a color value to each point in Rn. Thus, a continuous image is a function f from Rn (or a subset of Rn) to a color

space (RGB color model). For example, each pair of coordinates (x, y) can be assigned a red, green, and blue color (3-6) [10]:

$$R_r = f_r(x, y), \quad (3)$$

$$R_g = f_g(x, y), \quad (4)$$

$$R_b = f_b(x, y), \quad (5)$$

$$R_{x,y} = (R_r, R_g, R_b). \quad (6)$$

This image space model is powerful because analytical tools can be used for image processing.

For example, applying a red color filter to a rectangular area of the x, y image can be represented by:

$$\int_a^b \int_c^d f_r(x, y) dx dy \quad (7)$$

Image models as a set of vectors is particularly convenient for mapping operations in image space.

Another way to represent images in this way is to model the image as a set of vectors. Let V be a subset of vectors from R^n and let C be a color space. Then the subset $V \times C$ can represent the image. Each pixel in the image is represented by a vector indicating the location of that pixel and it is combined with . This indicates the color of that pixel. For example, ((25, -50), green) would represent a green pixel 25 units above and 50 units to the left of the origin. $v \in V, c \in C$

Let M be a set of color vectors representing images. To enlarge or reduce the image (known as uniform scaling St), you need to multiply each vector in M by a multiple of the identity matrix [10]. So:

$$S_t(M) = \left\{ \left[\begin{array}{cc} t & 0 \\ 0 & t \end{array} \right] v, c \mid (v, c) \in M \right\}, \quad (8)$$

where t is the scaling factor.

Similarly, the rotation of Ro is described as:

$$R_o(M) = \left\{ \left[\begin{array}{cc} \sin(o) & -\cos(o) \\ \cos(o) & \sin(o) \end{array} \right] v, c \mid (v, c) \in M \right\}, \quad (9)$$

where o is the angle of rotation.

With two images, it's easy to tell if one is an even scale of the other, that is, it is necessary to normalize both images in order to conclude that they are equal.

Basic expressions that describe operations in the image space, the following:

- horizontal scaling Sh (10);
- vertical scaling Sr (11);
- Cs image cropping (12):

$$S_h(M) = \left\{ \left[\begin{array}{cc} h & 0 \\ 0 & 1 \end{array} \right] v, c \mid (v, c) \in M \right\}, \quad (10)$$

$$S_r(M) = \left\{ \left[\begin{array}{cc} 1 & 0 \\ 0 & r \end{array} \right] v, c \mid (v, c) \in M \right\}, \quad (11)$$

$$C_s(M) = \left\{ \left[\begin{array}{cc} 1 & s \\ 0 & 1 \end{array} \right] v, c \mid (v, c) \in M \right\}, \quad (12)$$

where h is the horizontal scaling factor;

r— vertical scaling factor;

s— image crop factor.

Finally, an expression for all is obtained of reversible

linear transformations Ta,b,c,d [10]:

$$T_{a,b,c,d}(M) = \left\{ \left[\begin{array}{cc} a & b \\ c & d \end{array} \right] v, c \mid ac - bd \neq 0, (v, c) \in M \right\}, \quad (13)$$

V. APPLYING A FILTER FOR IMAGE PROCESSING

Further image processing is based on pixels in a small range (neighboring). This means that the transformed intensity is determined by the gray values at these points within the cols, and thus the enhancement of the spatial domain is also called cols operation or cols processing.

The filtering operation based on the spatial environment xy is called spatial domain filtering [11].

Red, blue, green filters

The filtering process consists in moving the filter point by point in the image function (6) so that the center of the filter coincides with the point (x, y). At each point (x, y), the filter response is computed based on the specific content of the filter and through a predefined relationship called a template.

If the pixel in the neighborhood is calculated as a linear operation (3), this is also called linear filtering of the spatial domain [11].

Some filters allow operations with the color tones of the image. The F1 color filter increases the intensity of the red, blue and green components of each pixel (3-5):

$$F_{1,x,y} = 1.2(R_r, R_g, R_b). \quad (14)$$

Thus, the color component of each pixel increased by 20% [12].

Monochromatic filter

Average method takes the average value of R, G and B as the value of gray gradations [13]:

$$F_2 = (R + G + B) / 3. \quad (15)$$

Theoretically, formula (15) is true by 100%. But at the time of writing software and program code execution uint8 overflow error occurs when processing images - the sum of R, G and B exceeds 255. To avoid overflow errors, R, G and B should be calculated accordingly:

$$F_2 = \frac{R}{3} + \frac{G}{3} + \frac{B}{3}. \quad (16)$$

The middle method is simple, but it doesn't work like that effectively, as expected. The reason is that people's eyes react differently to color model RGB. The eyes are most sensitive to green light, least sensitive to red light, and least sensitive to blue light. Since the three colors must have different weights in the distribution, then it leads to use weighted method.

Weighted method, also known as the luminance method, weights red, green, and blue according to their wavelengths [13]:

$$F_2 = 0.299R + 0.587G + 0.114B. \quad (17)$$

Object boundary detection filters

Object boundaries are usually one of the most important features of an image, so they are often used for measurements after applying a suitable filter. Thus, boundary detection is a very important stage of image preprocessing for any object

detection or recognition process. Simple boundary detection filters are based on the approximation of gradient images [14].

Operator Prewitt $F3x(x, y)$ and $F3y(x, y)$ can be represented as:

$$\text{for } F3x(x, y): \begin{matrix} -1 & 0 & 1 \\ -1 & 0 & 0, \\ -1 & 0 & 1 \end{matrix} \quad (18)$$

$$\text{for } F3y(x, y): \begin{matrix} -1 & -1 & -1 \\ 0 & 0 & 0. \\ 1 & 1 & 1 \end{matrix} \quad (19)$$

Operator Sobel $F4x(x, y)$ and $F4y(x, y)$ can be represented as:

$$\text{for } F4x(x, y): \begin{matrix} -1 & 0 & 1 \\ -2 & 0 & 2, \\ -1 & 0 & 1 \end{matrix} \quad (20)$$

$$\text{for } F4y(x, y): \begin{matrix} -1 & -2 & -1 \\ 0 & 0 & 0. \\ 1 & 2 & 1 \end{matrix} \quad (21)$$

Laplace operator $F5(x, y)$ is an approximation of the second-order derivative that determines the zero crossing. For example, the 3x3 Laplacian can be represented as:

$$\begin{matrix} 0 & 1 & 0 \\ 1 & -4 & 1. \\ 0 & 1 & 0 \end{matrix} \quad (22)$$

Magnitude and direction of the gradient.

The magnitude of the gradient the picture goes both ways $I_x(x, y)$ and $I_y(x, y)$. The gradient clearly defines the boundaries of the object. Whereas the gradient angle represents the direction of the edge or the direction of intensity change [14].

The magnitude of the gradient is defined as:

$$I_{xy} = \sqrt{I_x(x,y)^2 + I_y(x,y)^2} \quad (23)$$

The direction of the gradient is defined as:

$$I_0 = \tan^{-1} \frac{I_y(x,y)}{I_x(x,y)} \quad (24)$$

VI. IMAGE PREPROCESSING SOFTWARE

A software tool for the automated workplace of an ophthalmologist was developed to study the problems of diagnosing glaucoma. (Fig. 3).

The application is developed for the Android operating system. The developed image registration method provides:

1. receiving an image of the patient's face using a smartphone camera and identifying it with the built-in software of the operating system;
2. selection of areas of the left and right eye and placement of images in separate areas for detailed study;
3. scaling of images of the left and right eye (Fig. 4).



Figure 3. Software for the automated workplace of an ophthalmologist

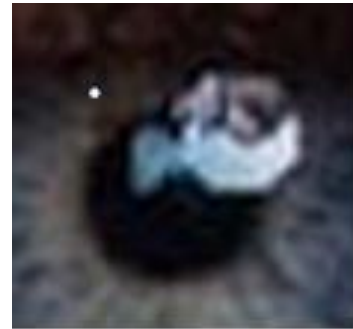


Figure 4. Scaling of left and right eye images

4. further processing to obtain images of the fundus with the use of filters (Fig. 5):

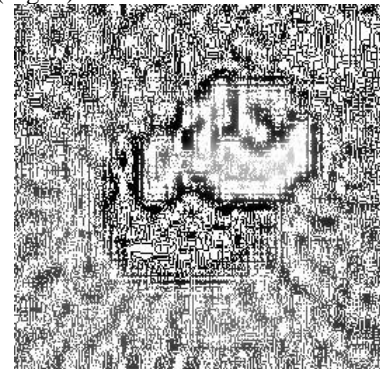


Figure 5. Further processing to obtain images of the fundus with the use of filters

CONCLUSIONS

1. An analytical review of the problems of diagnosing glaucoma in automatic mode was performed. It was found that one of the biggest problems in the diagnosis of glaucoma is the asymptomatic aspect of the disease before the severe stages. Thus, the number of undiagnosed patients exceeds the number of diagnosed patients. Processing of glaucoma images for the purpose of identification of pathology, its localization and analysis of the dynamics of changes in

automatic mode is an extremely important element of diagnostics.

2. A method of registering fundus images has been developed. The device that implements the method of obtaining, identifying and storing images of the fundus is a smartphone based on the Android operating system.

3. Mathematical models for describing fundus images are formalized. The image space model is powerful because analytical tools can be used to study images. Further image processing is based on pixels in a small range (neighboring). This means that the transformed intensity is determined by the gray values at these points within ca.

4. A software tool for the automated workplace of an ophthalmologist to study the problems of diagnosing glaucoma has been developed. The application is developed for the Android operating system. The developed method of image registration involves obtaining an image of the patient's face using a smartphone camera and identifying it with the built-in software tools of the operating system, selecting the areas of the left and right eye and placing the images in separate areas for detailed examination, scaling the images of the left and right eye, and further processing to obtain images fundus using filters.

ACKNOWLEDGMENT

This research has been funded by the Committee of Science of the Ministry of Science and Higher Education of the Republic of Kazakhstan (Grant No. AP 19675574).

REFERENCES

- [1] Global Prevalence of Glaucoma and Projections of Glaucoma Burden through 2040: A Systematic Review and Meta-Analysis. <https://www.sciencedirect.com/science/article/abs/pii/S0161642014004333>.
- [2] Ali N, Wajid SA, Saeed N, Khan MD. The relative frequency and risk factors of primary open angle glaucoma and angle closure glaucoma. *Pak J Ophthalmol.* 2007;23(3):117–21. <https://pjo.org.pk/index.php/pjo/article/view/766>.
- [3] International Council of Ophthalmology: Guidelines for glaucoma eye care. <http://www.icoph.org/downloads/ICOGlaucomaGuidelines.pdf>.
- [4] Boland MV, Ervin AM, Friedman DS, Jampel HD, Hawkins BS, Vollenweider D, Chelladurai Y, Ward D, Suarez-Cuervo C, Robinson KA. Comparative effectiveness of treatments for open-angle glaucoma: a systematic review for the US preventive services task force. *Ann Intern Med.* 2013;158(4):271–9. <https://www.acpjournals.org/doi/10.7326/0003-4819-158-4-201302190-00008>.
- [5] Divya L, Jacob J. Performance analysis of glaucoma detection approaches from fundus images. *Proc Comput Sci.* 2018;143:544–51. <https://linkinghub.elsevier.com/retrieve/pii/S1877050918321276>.
- [6] Burgoyne CF, Downs JC, Bellezza AJ, Suh J-KF, Hart RT. The optic nerve head as a biomechanical structure: a new paradigm for understanding the role of IOP-related stress and strain in the pathophysiology of glaucomatous optic nerve head damage. *Prog Retin Eye Res.* 2005;24(1):39–73. <https://linkinghub.elsevier.com/retrieve/pii/S1350946204000539>.
- [7] Zangalli C, Gupta SR, Spaeth GL. The disc as the basis of treatment for glaucoma. *Saudi J Ophthalmol.* 2011;25(4):381–7. <https://www.sciencedirect.com/science/article/pii/S1319453411000993?via%3Dihub>.
- [8] Machine learning applied to retinal image processing for glaucoma detection: review and perspective. <https://biomedical-engineering-online.biomedcentral.com/articles/10.1186/s12938-020-00767-2>.
- [9] Face detection guide. https://developers.google.com/mediapipe/solutions/vision/face_detector.
- [10] Mathematical Models of Image Processing. https://scholarship.claremont.edu/hmc_theses/188/.
- [11] Image Processing 101 Chapter 2.3: Spatial Filters (Convolution). <https://www.dynamsoft.com/blog/insights/image-processing/image-processing-101-spatial-filters-convolution/>.
- [12] The math that explains your photo filter. <https://www.matemagi.com/blog/the-mathematics-that-explains-your-photo-filter>.
- [13] Image Processing 101 Chapter 1.3: Color Space Conversion. <https://www.dynamsoft.com/blog/insights/image-processing/image-processing-101-color-space-conversion/>.
- [14] Image Filtering and Edge Detection. https://sbme-tutorials.github.io/2018/cv/notes/4_week4.html#edge-detection-kernels.
- [15] Orken Mamyrbayev, Sergii Pavlov, Oleksandr Karas, Iosip Saldan, Kymbat Momynzhanova, Sholpan Zhumagulova. Increasing the reliability of diagnosis of diabetic retinopathy based on machine learning, *Eastern-European Journal of Enterprise Technologies*, 2024/4/1, Том. 128. Выход. 9 . – DOI: 10.15587/1729-4061.2024.297849.